A low-frequency wideband metamaterial absorber based on a cave-disk resonator and resistive film*

Nie Yan(聂 彦), Cheng Yong-Zhi(程用志)†, and Gong Rong-Zhou(龚荣洲)

School of Optical and Electronic Information, Huazhong University of Science and Technology, Wuhan 430074, *China*

(Received 30 May 2012; revised manuscript received 28 August 2012)

A low-frequency wideband, polarization-insensitive and wide-angle metamaterial absorber (MA) is designed, simulated and analyzed. This MA consists of a periodic arrangement of a cave-disk resonator (CDR), square resistive film (RF), and metal ground plane (GP) (a 0.8 mm-thick FR-4 dielectric spacer is sandwiched in between the CDR and RF, and another 1.2-mm thick FR-4 dielectric spacer is inserted in between the RF and GP). The simulated results based on finite integration technology (FIT) indicate that the absorption of the MA is greater than 90% and almost perfectly impedance-matched to the free space in the whole frequency range of 1 GHz–7 GHz. The simulated absorptions under the conditions of different polarization and incident angles indicate that this composite structure absorber is polarization-insensitive and wide-angled. Furthermore, the distribution of the power loss density indicates that the wideband absorptivity is mainly from the composite electromagnetic loss of the CDR and RF. This design provides an effective and feasible way to construct a low-frequency wideband absorber.

Keywords: low-frequency, cave-disk resonator, resistive film

PACS: 41.20.Jb, 42.25.Ja, 78.20.Ci **DOI:** 10.1088/1674-1056/22/4/044102

1. Introduction

Electromagnetic (EM) metamaterials (MMs) are artificially structured materials that may exhibit many exotic properties that are not present in natural materials, such as negative refractivity,[1,2] a reversed Doppler shift,[3] reversed Cherenkov radiation,[4] and superlenses,[5] cloaks,[6] and perfect absorption.[7,8] Essentially, MM is an artificially structured material which attains its properties from the unit structure (its scale is much smaller than the wavelength of interest) rather than the constituent material. That is to say, MM is also a concept of material design. In the past decade, the research field of MMs in science and technology has covered a vast range, including the structure and EM properties. Much attention has been paid to the design and application of MMs, due to their designable and controllable material parameters, such as effective permittivity ($\varepsilon_{\rm eff}$), and permeability ($\mu_{\rm eff}$). Thus, MMs are believed to hold great promise for future applications.

Since Engheta[9] first proposed the theoretic view of using metamaterial to achieve a perfect absorption for EM waves, and Landy *et al*.[7] first conducted microwave experiments to demonstrate this, research on absorption in EM waves has become an important aspect in the research of MMs. The perfect absorption of MM is mainly due to the local EM resonance mechanism, that is to say, from the resonance between dielectric loss and impedance matching. Based on this resonance mechanism, from the microwave region to the visible light region, various metamaterial absorbers (MAs), each consisting of two or more layers coupling sandwiched resonance structures, have been proposed and investigated widely.[6,7,9–14] However, the strong absorption bandwidth is very narrow, which may impede its application in practice.

Recently, based on the concept of MM resonance absorption, several attempts to achieve broadband strong absorption have been made, especially in a gigahertz frequency region.[15–24] Besides its polarization and incidence angle dependence, the bandwidth of MA is an important aspect that may affect many applications. In particular, the low-frequency bandwidth is difficult to extend without increasing the substrate thickness significantly. Gu S *et al*.[16] and Gu C *et al*.[17] proposed electric resonator structure MA loaded lumped elements. The equivalent circuit model was also used to introduce the working principles of the narrowband and the wideband absorbing structure loaded high impedance surfaces by Filippo *et al*.[18] and Pang *et al*.[19] Sun *et al*.[20] proposed a composite structure MA based on an electric resonator structure and resistive patches, which exhibits a stronger low-frequency absorption. In the present paper, the concept of MM was also employed to design, simulate, and analyze a low-frequency wideband MA without increasing the total thickness significantly. Theoretical and simulated results show that this composite structure MA has a polarization-insensitive and wide-angle absorption from 1 GHz to 7 GHz. This design provides an effective way to construct low-frequency wideband absorbers with high performance in stealth technology, and also theoretic support for the ongoing experiment.

*Project supported by the National Natural Science Foundation of China (Grant No. 51207060) and the Specialized Research Fund for the Doctoral Program of Higher Education of China (Grant No. 20090142110004).

†Corresponding author. E-mail: cyz0715@126.com

© 2013 Chinese Physical Society and IOP Publishing Ltd

2. Design and simulation

For the MA, the expression of the absorption is $A(\omega) = 1 - T(\omega) - R(\omega) = 1 - |S_{21}|^2 - |S_{11}|^2$, where $A(\omega)$, S_{11}, and S_{21} are the absorption, reflection coefficient, and transmission coefficient each as a function of frequency ω. In the case without transmission and reflection, ideally it will result in total absorption. For our proposed MA, there is no transmission to be observed since the ground plane (GP) thickness is greater than the skin depth of copper in this frequency range. Only the reflection needs to be examined. Thus, the absorption is calculated by the equation $A(\omega) = 1 - |S_{11}|^2$.

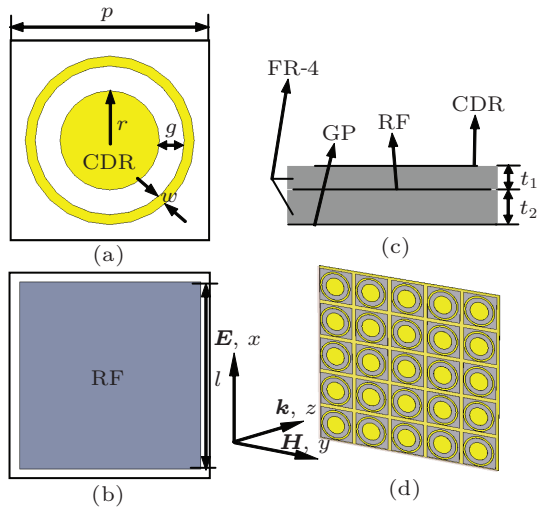


Fig. 1. (color online) Schematic diagram of the MA unit cell: (a) cave-disk structure electric resonator, (b) square resistive film, (c) side view of the unit cell of the MA, (d) three-dimensional array model.

Our previous investigations indicated that the MA only consists of a dielectric substrate sandwiched with an electric resonator structure and metal GP, which is mainly due to the local EM resonance and impedance matched characteristics,[8,11,15] and so it is difficult to achieve broadband strong absorption. Even the bandwidth of the absorption can be improved by using a multi-electric resonator structure in a co-planar.[15] The bandwidth improvement is limited. The MA based on a resistive film (RF) could achieve broadband absorption, however, it is difficult to obtain a high absorbing performance in a low-frequency range.[18,19] To achieve a stronger absorption in a low-frequency wideband, a composite structure MA model is designed, as shown in Fig. 1. The MA unit cell consists of a cave-disk resonator (CDR), an RF, an FR-4 dielectric spacer, and a GP from top to down, as shown in Fig. 1(c). We select FR-4 (loss) with the relative dielectric constant $\varepsilon_r = 4.9$ and the loss tanδ=0.025 as the dielectric spacer. The CDR structure and continuous metal GP are selected to be copper, whose conductivity is $\sigma = 5.8 \times 10^7$ S/m and thickness is $t_m = 0.035$ mm. The thickness and surface resistance of the square resistive films are 0.15 mm and 125 kΩ/sq, respectively. The optimal parameters for the unit cell structure are as follows (in millimeters): $p = 20$, $w = 1$, $r = 5$, $g = 2.5$, $l = 19$, $t_1 = 0.8$, and $t_2 = 1.2$. Based on the design of the unit cell of the composite structure MA, to demonstrate the microwave absorption, a full wave EM simulation is performed based on the finite integration technology (FIT) with CST Microwave Studio software. In the simulation, the electromagnetic wave $\boldsymbol{k}$ is incident on the z axis, with the magnetic field $\boldsymbol{H}$ being parallel to the y axis and the electric field $\boldsymbol{E}$ being parallel to the x axis, and the periodic boundary conditions are used in the x and y directions in order to obtain periodicity in the transverse plane. Rapid convergence to a nearly optimal design could be achieved readily.

3. Results and discussion

The simulated reflection and absorption properties of MA are shown in Fig. 2(a). As shown in Fig. 2(a), in a frequency range from 1 GHz to 7 GHz, the reflection is lower than 10%, and the corresponding absorption exceeds 90%. To better understand the principle of the high absorption, the relative wave impedance ($\tilde{z}(\omega)$) for the normal incidence is retrieved from the simulated S parameters[12], as shown in Fig. 2(b). The real part of relative impedance is nearly unity (Re$(z) \approx 1$) and consistent with what we want to match, the impedance of the free

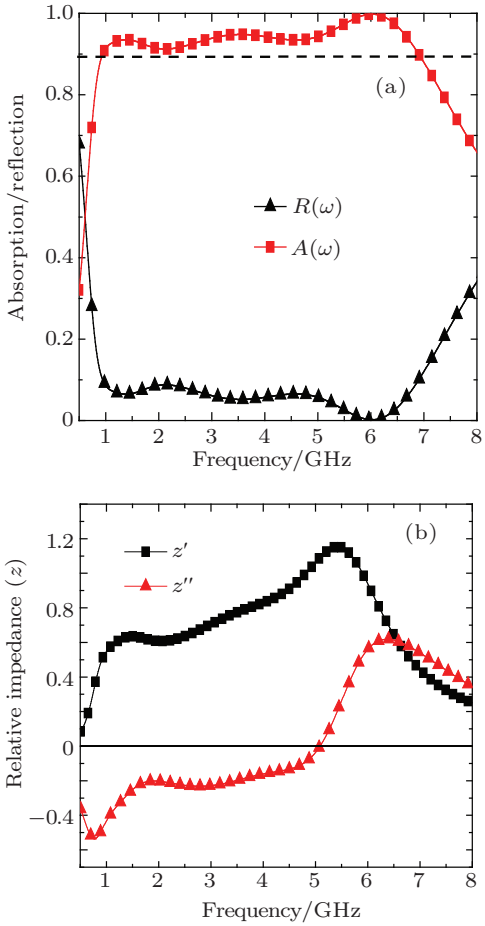


Fig. 2. (color online) Simulated results of (a) reflection and absorption, and (b) the corresponding relative impedance.

space from 1 GHz to 7 GHz, and the imaginary part is minimized ($\mathrm{Im}(z) \approx 0$), which means that the reflection is nearly zero. These results indicate that the impedance of our MA can be tuned to approximately match the impedance of the free space in a wideband absorption frequency range.

In the above discussion, the absorption was obtained under normal incidence. In practical use, EM waves are usually incident onto absorbers with a different polarization angle or oblique incidence angle, so it is necessary to examine the absorption under different polarization angles and oblique incidence angles. As shown in Fig. 3, we analyze the influence of the incident condition on the absorption property of MA. From Figs. 3(a) and 3(b), owing to the high symmetry of the unit cell, the absorptions under different polarization angles are unchanged for the transverse electric (TE) and transverse magnetic (TM) waves. Figures 3(c) and 3(d) show the simulated absorptions of our MA at various angles of oblique incidence for the TE and TM configurations. For the TE wave oblique incidence, the absorption is nearly unchanged below 60° in a frequency range from 1 GHz to 7 GHz. However, beyond 60°, there is a sudden decrease in the absorptivity, as the y component of the incident magnetic field decreases rapidly to zero and can no longer efficiently excite this magnetic polariton.[13,15] For the case of the TM wave, the absorption will be nearly unchanged with the increase in incidence angle in a wideband frequency range, due to the fact that the composite structure can be effectively excited by the magnetic field. These results indicate that the MA is polarization-insensitive and wide-angled.

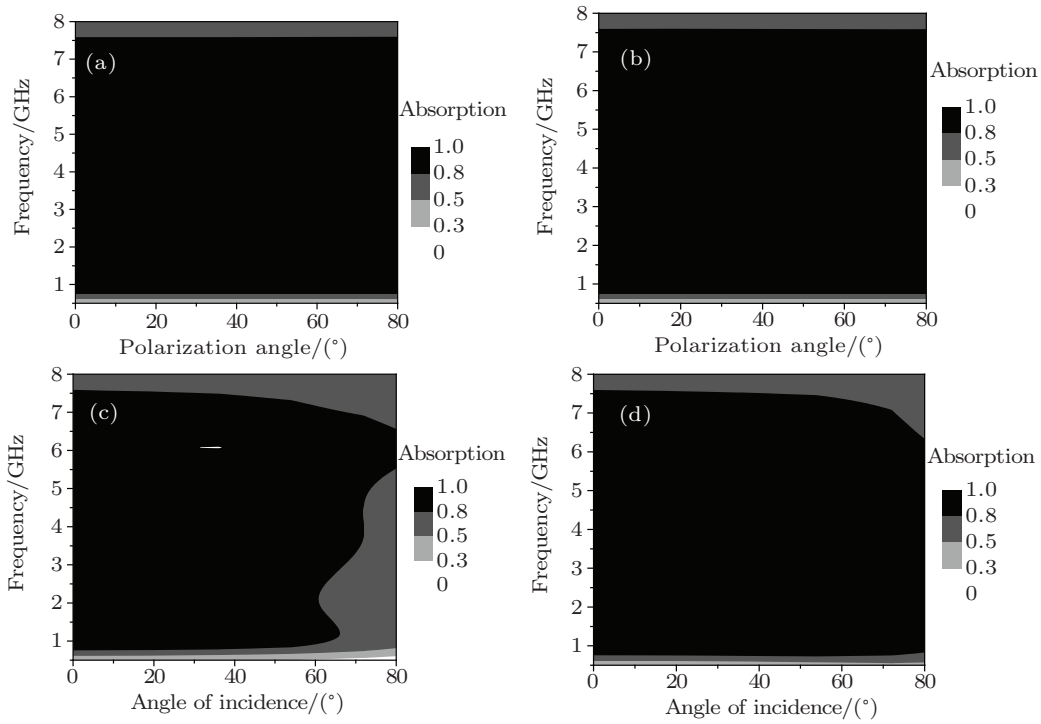


Fig. 3. Simulated absorptions with different polarization angles under normal incidence: (a) TE; (b) TM. Simulated absorptions at different angles of incidence: (c) TE; (d) TM.

To further better understand the wideband absorbing properties of the designed composite MA, we should study the absorptions of the CDR absorber and RF absorber, as shown in the insets of Fig. 4, respectively. From Fig. 4, the CDR absorber consists only of a CDR and GP separated by the FR-4 dielectric substrate with a thickness of 1 mm, and the other parameters are kept the same as those of the above composite MA. It can be observed that there are two absorption peak values of 96.5% and 99.7% at 3.1 GHz and 7.45 GHz, respectively. To better understand the physics behind it, in Figs. 5(a)–5(c) the distributions of the power loss densities at different frequencies of the MA are examined. As shown in Fig. 5(a), the strong power loss of the lower frequency (3.1 GHz) mainly concentrates on the up and down sides of the outer ring of CDR, and the maximum value is up to 4.85×10^6 (W/m^3). Similarly, the power loss of the higher frequency (7.45 GHz) mainly concentrates on the up and down sides of the inner disk of CDR and the maximum value is up to 1.28×10^7 (W/m^3), as shown in Fig. 5(b). The power loss in the other off-resonant area is very weak. The perfect absorptions of both the lower and higher frequency resonance are caused primarily by the excitation of the electric dipole resonance and the strong magnetic coupling, simultaneously.[15] On the other hand, at off-resonant frequency (e.g. 7 GHz), the absorption is very small, and the corresponding maximum power loss value is only 55763 (W/m^3) (see Fig. 5(c)), which is much less than the

maximum value at resonant frequency.

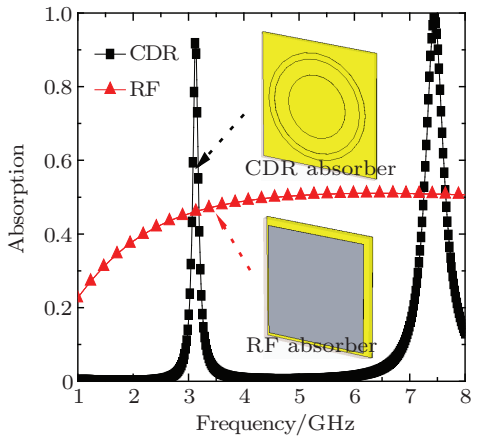


Fig. 4. (color online) Simulated absorptions of the CDR (solid square line) and RF (solid triangle line) absorbers.

Taking a further step, we study the RF absorber, which consists only of a square RF sandwiched with an FR-4 dielectric substrate of 2 mm in thickness and a GP (see the inset of Fig. 4). The structural parameters are kept the same as those mentioned above, and the simulated absorption is shown in Fig. 4. It is clear that the overall absorption spectrum is almost flat and the absorption is below 50%, which is mainly due to surface resistive loss and strong magnetic coupling.[15,18] That is to say, the low absorption of overall frequency is mainly caused by the weaker electric resonance and stronger magnetic resonance simultaneously, resulting in relative wave impedance mismatching to the free space.[10,12,18] To obtain an insight into the physical picture of the intriguing absorbing features of the RF absorber, the power loss density distributions at different frequencies are also calculated, and the results are shown in Figs. 5(d)–5(f). It can be observed that there are similar power loss density distributions at different frequencies of 2, 4, and 6 GHz, and the power losses all concentrate on the up and down edges of the square RF. The corresponding maximum values of power loss are 1.29×10^5 (W/m^3), 96523 (W/m^3), and 1.31×10^5 (W/m^3), which are much less than the maximum values of the resonant frequency of the CDR absorber. These results are very consistent with the corresponding absorptions of the CDR and RF absorbers.

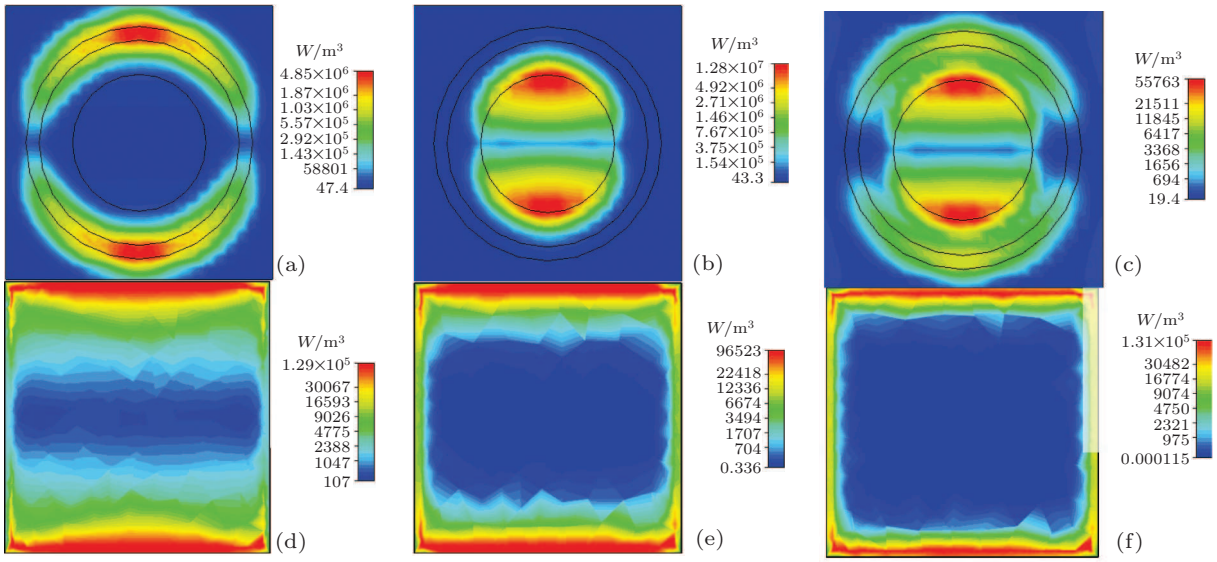


Fig. 5. (color online) Distributions of the power loss density of the CDR and RF absorbers at different frequency points: (a) 3.1 GHz, (b) 7.45 GHz, and (c) 7 GHz for the CDR absorber; and (d) 2 GHz, (e) 4 GHz, and (f) 6 GHz for the RF absorber.

From the above studies, we can conclude that it is difficult for the MA based on CDR or RF to achieve low-frequency and wideband high absorptance. However, there are some advantages for either CDR or RF, e.g. the CDR absorber could achieve stronger narrowband absorption, and the RF absorber could possess wideband properties. Thus, this inspired us to construct a low-frequency wideband high-performance absorber based on CDR and RF assembly without significantly increasing the thickness. Due to this inspiration, we designed a composite structure MA, which is shown in the inset of Fig. 6(a). It is also interesting to explore the power loss in the MA since it can provide information about how and where the absorption happens. Figure 6(a) shows absorptions under two different loss conditions. When an FR-4 substrate is lossy, the absorption exceeds 90% in a frequency range from 1 GHz to 7 GHz and the absorption relative bandwidth of the central frequency is up to 150%. When the FR-4 substrate is loss-free, the absorption in a frequency range from 1 GHz to 7 GHz is almost the same as that under lossy conditions. These results indicate that the wideband high absorption is mainly due to a resistive film and cave-disk resonator. To further illuminate the absorbing features of this composite MA, the distributions of the power loss density at different frequencies are also calculated. Here, to make a clearer illustration

of the point, we only choose two typical frequencies (a lower frequency of 1.2 GHz and higher frequency of 6.1 GHz) to simulate the distributions of the power loss density. As shown in Fig. 6(b), it can be clearly seen that the strong power loss of the lower frequency (1.2 GHz) mainly focuses on the up and down part of the surface of MA, and the maximum value is up to 7.11×10^5 (W/m^3). The area of the power loss distributions is much larger than the corresponding areas of the CDR and RF absorbers (see Figs. 5(a) and 5(d)). Similarly, for higher frequency (6.1 GHz), in Fig. 6(c), the strong power loss mainly focuses in the middle of the up and down parts of the surface of MA, and the maximum value is up to 9.25×10^5 (W/m^3). The power loss distribution area is much larger than the corresponding areas of the CDR and RF absorbers (see Figs. 5(b) and 5(e)) as well.

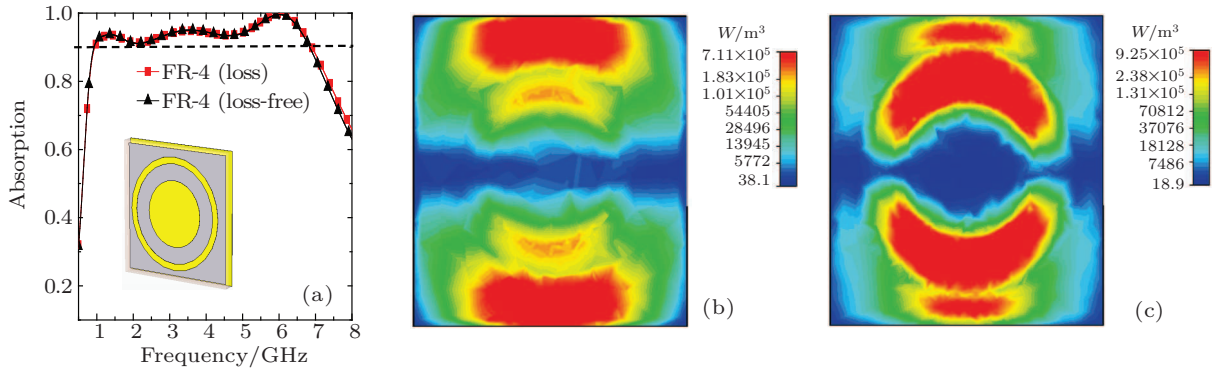


Fig. 6. (color online) (a) Absorptions of composite structure MA under two different loss conditions, and the power loss density distributions of the designed composite structure MA at different frequencies of (b) 1.2 GHz and (c) 6.1 GHz.

From the above physical pictures of the intriguing absorbing features, we can conjecture that the low-frequency high absorbing property is caused mainly by the strong electric resonance and stronger magnetic resonance, simultaneously, resulting in the impedance matching to the free space in a wideband frequency range.[10,12,18–20] On the other hand, the influence of the RF on the wideband high absorption of the composite MA is also very important.[18–20]

4. Conclusion

In the present study, we propose a thin, low-frequency, wideband, polarization-insensitive and wide-angle metamaterial absorber according to CDR and RF. This absorber is not limited to the minimum thickness of a quarter wavelength, and it is very thin: the whole thickness is only 2 mm (about 1/32 of the center operation wavelength). The simulation results show that the absorber has a low-frequency wideband strong absorption for the incident wave in a frequency range from 1 to 7 GHz. The simulation absorptions under different polarization angles and oblique incidence angles indicate that the MA is polarization-insensitive and wide-angled. Further simulation absorptions and power loss density distributions of different types of MAs indicate that the stronger low-frequency wideband absorption of the composite structure MA is mainly due to the composite electromagnetic losses of CDR and RF. This MA is fabricated easily in experiments. The CDR layer can be fabricated by conventional PCB technology or standard optical lithography processes. The RF layers are usually fabricated by silk-screen printing of resistive slurries into a pattern on a dielectric substrate backed by a grounded plane. This design provides the theoretic support for the ongoing experiment.

References

[1] Veselago V G 1968 *Sov. Phys. Usp.* **10** 509
[2] ShelbyR A, Smith D R and Schultz S 2001 *Science* **292** 77
[3] Seddon N and Bearpark T 2003 *Science* **302** 1537
[4] Grbic A and Eleftheriades G V 2002 *J. Appl. Phys.* **91** 5930
[5] Pendry J B 2000 *Phys. Rev. Lett.* **85** 3966
[6] Schurig D, Mock J J, Justice B J, Cummer S A, Pendry J B, Starr A F and Smith D R 2006 *Science* **314** 977
[7] Landy N I, Sajuyigbe S, Mock J, Smith D R and Padilla W J 2008 *Phys. Rev. Lett.* **100** 207402
[8] Cheng Y Z, Xiao T, Yang H L and Xiao B X 2010 *Acta Phys. Sin.* **59** 536 (in Chinese)
[9] Engheta N 2002 *IEEE Anten. Propag. Soc. Int. Symp.* **2** 92
[10] Avitzour Y, Yaroslav A, Urzhumov and Shvets G 2009 *Phys. Rev. B* **79** 045131
[11] Lockyear M J, Hibbins A P, Sambles J R, Hobson P R and Lawrence C R 2009 *Appl. Phys. Lett.* **94** 041913
[12] Cheng Y Z, Yang H L, Cheng Z Z and Xiao B X 2011 *Photon. Nanostruct. Fundam. Appl.* **9** 8
[13] Grant J, Ma Y, Saha S, Khalid A and Cumming D R S 2011 *Opt. Lett.* **36** 3476
[14] Ding P, Liang E, Cai G, Hu W Q, Fan C Z and Xue Q Z 2011 *J. Opt.* **13** 075005
[15] Luo H, Cheng Y Z and Gong R Z 2011 *Eur. Phys. J. B* **81** 387
[16] Gu S, Barrett J P, Hand T H, Popa B I and Cummer S A 2010 *J. Appl. Phys.* **108** 064913
[17] Gu C, Qu S B, Pei Z B, Zhou H, Xu Z, Bai P, Peng W D and Lin B Q 2010 *Chin. Phys. Lett.* **27** 117802
[18] Filippo C, Agostino M and Giuliano M 2010 *IEEE Trans. Anten. Propag.* **58** 1551
[19] Pang Y Q, Zhou Y J and Wang J 2011 *J. Appl. Phys.* **110** 023704
[20] Sun L K, Cheng H F, Zhou Y J and Wang J 2011 *Appl. Phys. A: Mater. Sci. Process.* **105** 49
[21] Yang Y J, Cui Y J, Wen G J, Zhong J P, Sun H B and Oghenemuero G 2012 *Chin. Phys. B* **21** 038501
[22] Cheng Y Z, Wang Y, Nie Y, Gong R Z, Xiong X and Wang X 2012 *J. Appl. Phys.* **111** 044902
[23] Sun L K, Cheng H F, Zhou Y J and Wang J 2012 *Chin. Phys. B* **21** 055201
[24] Cheng Y Z, Nie Y, Gong R Z, Zheng D H, Fan Y N, Xiong X and Wang X 2012 *Acta Phys. Sin.* **61** 134101 (in Chinese)